INVESTIGATION OF AN ANOMALOUS FAILURE OF BEARING ON A FAN WITHIN THE COLUMBUS MODULE OF THE ISS

G. Parzianello[(1)], M. Schmid[(2)], E. Roberts[(3)], O. Duforet[(4)]

[(1)]ESA/ESTEC, Keplerlaan 1, Postbus 299, 2200 AG – Noordwijk (NL), Email:giorgio.parzianello@aoes.com
[(2)] ASTRIUM GmbH, 88039 Friedrichshafen (D), manfred.schmid@astrium.eads.net :
[(3)] ESTL ESR Technology, Whittle House, Birchwood Park, Risley, Warrington (UK), Email:emyr.roberts@esrtechnology.com:
[(4)]SOTEREM 5 rue de la technique, F-31320 CASTANET-TOLOSAN (France), Email: olivier.duforet@soterem.fr:

ABSTRACT

A premature failure of an Inter module Return Fan Assembly (IRFA) within the Columbus module of the International Space Station (ISS) has been investigated to identify the root cause and the counteractions to be taken. The dismounted parts and the collected debris have been analysed using optical microscopy, Scanning Elecron Microscopy (SEM), Energy Dispersive spectroscopy (EDS) and dedicated dimensional measurements have been performed.
The inspection indicated an anomalous wear of one only of the two support bearings and in particular a strong interaction between the cage and the lands of the outer ring with consequent friction and wear, while the other parts of both the bearings were in reasonable conditions.
The analyses indicated a misalignment of one bearing this being the origin of the non-nominal load conditions that led to the premature wear of the bearing. The inspections conducted allowed the identification of the corrective actions to be implemented in order to minimize the likelihood of occurrence of the failure.

1 INTRODUCTION

The Ventilation and Air Conditioning system of the Columbus module of the International Space Station (ISS) includes cabin air and intermodule ventilation, air filtering, air temperature and humidity control and monitoring of air composition. The air flow through the module is provided by the Inter Module Ventilation (IMV) composed of the Inter module Supply Fan Assembly (ISFA) and the Inter module Return Fan Assembly (IRFA). To improve the air circulation two additional fans are also provided (Cabin Fan Assemblies CFA). In Figure 1 the scheme of the ventilation system is depicted.
All the fans in the ventilation system (ISFA, IRFA CFAs) share the same design of the motor and bearing assembly.

An anomalous behaviour was observed onboard for the IRFA after few months from the beginning of operations. The observed anomaly comprised high peaks in the current drawn by the malfunctioning fan accompanied by higher-than-expected noise. In a relatively short period of time (about 15 days) the behaviour worsened to become very noisy and unstable in current consumption. An initial onboard troubleshooting activity confirmed the different behaviour of the IRFA compared to the other fans onboard and pointed towards a possible bearing failure within the IRFA unit, causing higher motor current absorption, significantly louder noise and temperature increases.
The poorly performing fan was therefore switched off and returned to Earth for investigation of the failure and fault analyses. The incoming checks and left hand bearing inspection have been performed by SOTEREM, while the right hand bearing has been inspected by ESTL and ESTEC.

The bearing assembly of the IRFA fan consists of two angular contact bearings mounted with a compliant preload given by wavy washers. In this configuration the right bearing has to be free to slide axially in the housing in order to maintain the design preload in case of thermal gradients, while the left bearing is fixed. The preload of the bearing assembly is 105 N
The following Figure 1 shows the scheme of the ventilation system and a section of the motor assembly

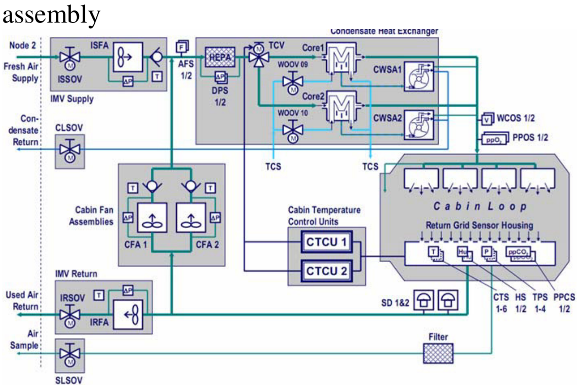

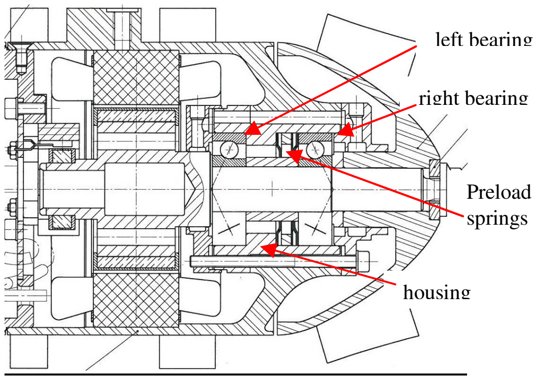

Figure 1: Scheme of the ventilation system and motor assembly

2 INVESTIGATION OF THE LEFT HAND BEARING

2.1 Incoming test

A functional and performance test at a defined and known performance point (8400 rpm) was performed. After 23 minutes, the test was stopped due to high current peaks and temperature increases. The motor current consumption was slightly higher than the nominal but remained constant during 20 minutes. Afterwards peak consumption and average consumption increases brought the test to a stop (see Table 1)

Table 1: Incoming performance check

	Previous test (acceptance 2003)	Incoming test (2009)
Motor Current	0.82 A	From 0.86 to 1.2 A
Motor Temp	23°C	28°C

A verification of the fan static torque showed a high value (around 0.52 Nmm against the nominal 0.07-0.08 Nmm). The torque along one turn was not constant and some positions of higher resistive torque were distinguishable.

The failure of the IRFA fan was confirmed at the motor level, due to mechanical issues.

2.2 Fan disassembly

After separation of the motor from the aerodynamics items and dismounting of the motor subassembly, the grease within and around the bearing showed a brownish aspect, with a very high viscosity. Figure 2 shows the general aspect of the bearing with the "dried" grease.

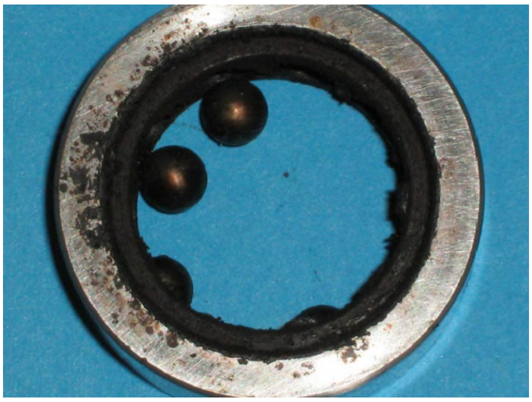

Figure 2: Left hand bearing (without inner ring)

Other evidences noticed when disassembling were :

- Some dust particles were found around the blade of the fan but the internal motor parts were clean.
- There were some indications that a particle brought by the airflow had impacted the impeller of the fan and had become jammed between one rotating blade and the fix casing. This had generated a slight groove on the casing.
- There were some rotational friction marks on the motor shaft and impeller (eventually related to the previous evidence), caused by complete or partial jamming of the impeller.

The bearing preload is generated by 6 washer springs; the load is adjusted during integration process by a dedicated shim.

After verification of the spring stiffness and the dimension of the shim, it was confirmed that the generated bearing load matched the expected value (105 N).

2.3 Left hand bearing inspection

The ball raceways, when observed with a binocular optical magnifier, appeared to have a brownish colouration in the inner and outer rings (Figure 3). This condition had been generated possibly by lack of lubricant capability or high load over a short time period.

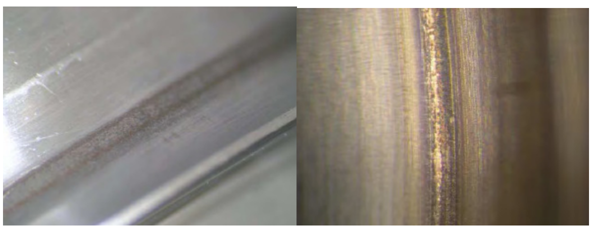

Figure 3: Inner ball race (left) and outer ball race (right)

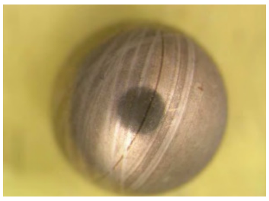

Figure 4: View of ball with marks

Scanning Electron Microscopy (SEM) observations did not indicate abnormal wearing of the inner and outer ring's ball raceways or of the phenolic cage

Some marks on the surface on the balls were observed (Figure 4). The traces were not measurable by a high accuracy profilometry method, thus indicating a high load event of short duration

2.4 Chemical analysis of the grease

As all the grease was found to be in the same darkened condition, some chemical analyses were performed to check the possibility that a severe common environmental factor could have been a root cause for the grease degradation.

The technique of Fourier Transformed InfraRed spectroscopy (FTIR) was used to compare chemical bonding between samples.

Different tests performed by FTIR in reflection mode and transmission mode, with samples coming from the inspected IRFA bearing and from the original grease batch used for fan integration,, were performed. No significant difference between the batches was detected The IRFA grease did not appear to be chemically modified (no important pollution, no molecular bonding change).

3 INVESTIGATION OF THE RIGHT BEARING

The right bearing could be rotated readily by hand but did not spin freely. The cage, which was designed to be outer-race riding, appeared a fairly close fit (small gap) with the outer race lands (Figure 5a). Where visible, the grease in the assembled bearing appeared brownish in colour – indicating the possible presence of phenolic cage debris and/or oxidised steel debris. The end face of the outer ring on the non-relieved side exhibited some patches of dark discolouration (Figure 5b). There was one reddish-brown corrosion mark (Figure 5c) present on the OD of the outer ring. A corresponding corrosion mark (mirror image) was found on the bearing housing (Figure 5d).

The bearing was dis-assembled and the separated parts were examined by optical microscopy. There was blackened (greyish black) grease over much of the inner race surface (Figure 6a). The bore of the inner race appeared free of grease and relatively clean. Black-coloured grease was also present in the outer ring race (Figure 6b) and there were also reddish-brown patches present.

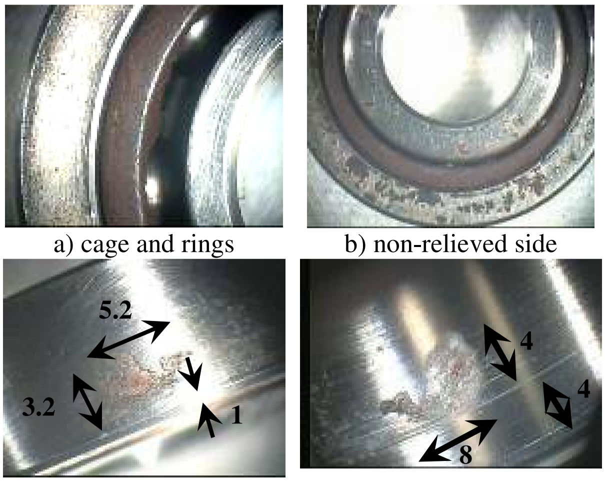

a) cage and rings b) non-relieved side

c) Corrosion on outer race d) corrosion feature on bearing housing

Figure 5: Images of the right hand bearing and housing. Dimensions in mm

The lands of the outer race showed distinct circumferential wear marks in the steel which appeared bright and shiny (Figure 6b). The corresponding surfaces of the cage were heavily worn (Figure 7) in some areas and a distinct step could be seen between the worn and unworn (central) part. Clearly such cage wear was indicative of strong cage-to-land interactions.

a) Inner race b) Outer race

Figure 6: Images of bearing parts after dis-assembly

There were heavy wear marks within the cage pockets indicating high ball-to-cage forces had occurred. The balls displayed patches of hard ('caked'), blackened grease and had areas of reddish brown appearance: the latter probably caused by transfer of phenolic material from cage to ball during ball-to-cage interactions.

3.1 Observations of cleaned bearing parts with optical microscopy

In an attempt to remove grease and debris, selected bearing parts were subjected to ultrasonic solvent cleaning for a period of 5 mins. The solvent was then filtered in order to recover particulate matter.

Cage
The wear on the OD (outer diameter) of the cage varies with circumferential position. The position of greatest cage wear (about 0.15 mm) is shown in Figure 7a and that of least wear (about 0.02 mm) in Figure 7b.

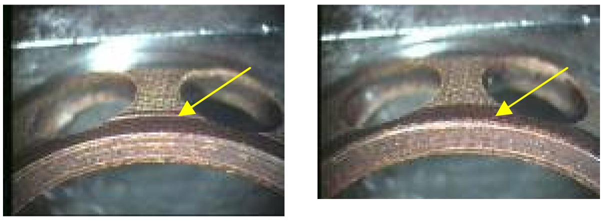

a) Largest wear step b) Smallest wear step

Figure 7: Images of cleaned cage

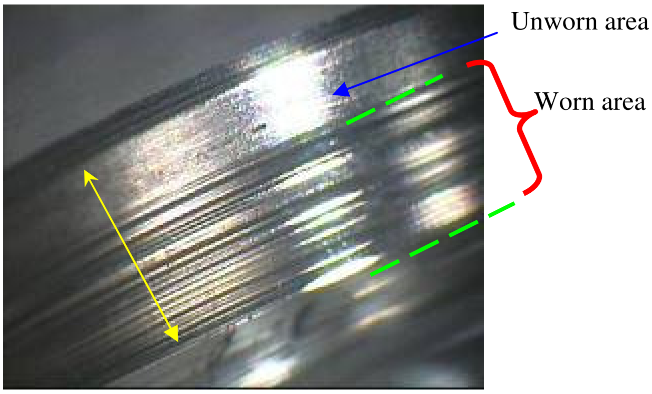

Figure 8: Wear grooves on land of outer ring. In yellow the entire width of the land

Outer ring
Solvent cleaning removed most of the black-coloured debris but there remained brownish patches within the raceway. The circumferential wear marks on the land appeared clearly visible as grooves not extending for the entire width of the land (Figure 8). Both lands exhibited wear of this nature. The ball track was not clearly discernible. There remained the corrosion mark on the OD (Figure 9a). The debris filtered from the solvent is shown in Figure 9b.

a) Corrosion OD of outer ring b) Debris collected from outer ring

Figure 9: corrosion on OD of outer ring (left) and debris recovered from solvent used to clean outer ring (right)

The appearance of circumferential marks on the bearing housing and on the outer ring corresponding to the corroded mark (Figure 10) suggested that rotation of the outer ring within the housing had, at some stage, taken place.

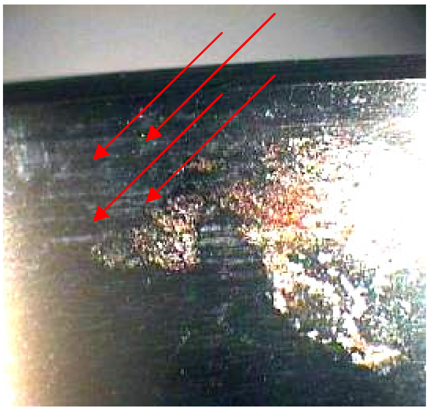

Figure 10: circumferential lines passing through corroded area

Inner ring
A clear, rather narrow, reddish brown ball track was visible (see Figure 14). The track had a uniform width and appeared to be square to the bearing axis.

Balls
The surface of the cleaned balls had a slightly matt finish and in close-up had an 'orange peel' appearance but appeared not particularly damaged.

3.2 SEM/EDAX examinations

These examinations focussed on:
- the corroded area on the OD of the outer ring
- wear debris (collected after filtration of the solvent used to clean the outer ring)
- worn areas of cage

As there was unequivocal evidence that the bearing contained phenolic and bearing steel debris it was appropriate to start the SEM/EDAX examination by obtaining elemental signatures of these two materials. The bearing race steel has the designation Z100 CD17 and has the composition shown in

Table 2. Table 3 indicates the composition of the housing steel (15-5PH H1025 steel).

Table 2: Bearing steel composition

Weight %	**C**	**Si**	**Mn**	**P & S max**	**Cr**	**Mo**	**Ni**	**Others**
Z100CD17	0.90/1.2	1.0 max	1.0 max	0.04 P 0.03 S	16.0 / 18.0	0.35 / 0.75	0.50 max	Cu 0.50 max

Table 3: housing steel composition

Weight %	C	Si	Mn	P & S max	Cr	Cu	Ni	Nb + Ta
15-5PH H1025	0.07 max	1.0 max	1.0 max	0.04 P 0.03 S	14.0 / 15.50	2.50 / 4.50	3.50 / 5.50	0.10 / 0.45

The EDAX spectrum appeared consistent with the expected composition of the bearing steel with clear peaks corresponding to Fe, Cr, Si, C and Mo present. A weak signal corresponding to Ni was discernible but those for Cu and Mn were not.

The phenolic cage was specified to be manufactured from material having the designation Spaulding T-346-TR. T-346, a fine-weave, cotton-linen phenolic thermally treated to give additional dimensional stability. The spectrum from the phenolic cage did show strong signals from carbon and oxygen as expected. In addition there were peaks corresponding to silicon and aluminium.

3.3 OD of outer ring (corrosion mark)

SEM images of the corroded area are shown in Figure 11. The EDAX spectrum corresponding to this area displayed the expected peaks of iron, chromium, molybdenum, carbon and silicon which are inherent to the bearing steel and also relatively strong signals from nickel and copper which are minor constituents of the steel's composition (Table 1) but which were not apparent in the spectrum from the uncorroded steel. This could be related to the higher Ni content of the housing steel, and the interactions among the two parts

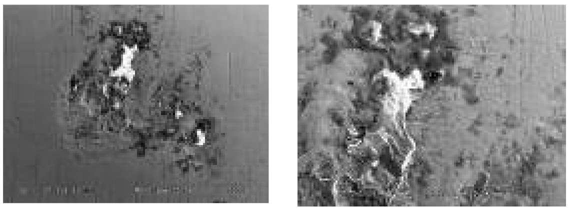

Figure 11: SEM images of corroded surface on OD of outer ring

3.4 Wear debris from outer ring and cage

Some of the wear debris filtered from the cleaning of the bearing's outer ring was examined by SEM. Figure 12 shows an SEM image of typical debris and the elements identified using EDAX analysis are shown in Table 4.
Based on the EDAX signatures obtained from the raw cage and ring material we have attempted to identify the composition of the particles (final column,Table 4).
The worn area of the OD of the cage was also examined by SEM in order to determine whether there was any embedded steel wear debris present. The results indicated conclusively that steel debris was present and embedded in the cage

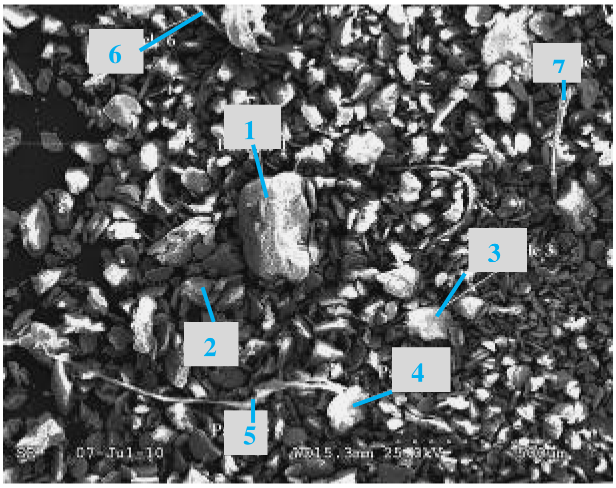

Figure 12: SEM micrograph of debris recovered form outer ring

Table 4: Identified elements on debris using EDAX analysis

Particle No.	Elements in order of EDAX signal strength	Approximate particle size (µm)	Likely source of particle
1	C, Fe, Cr, O, Si	350 x 250	Phenolic + steel
2	Fe, Cr, C, O, Si	100 x 50	Steel + phenolic
3	Fe, Cr, C, O, Si	150 x 100	Steel + phenolic
4	Fe, Cr, C, O, Si	150 x 100	Steel
5	C, Fe, Cr, O, Si	Fibre	Cotton fibre
6	C, Cl, K, Fe, Na, O, Pd	Fibre	Contaminated cotton fibre
7	C, Fe, Cr, Si, Cl	Fibre	Cotton fibre

4 ADDITIONAL INVESTIGATION OF THE RIGHT BEARING

After the aforementioned inspections and analyses some observations remained not fully explained, therefore some additional dedicated inspections were carried out.
The main points to be clarified can be summarized in the following:

- Absence of balls track on the outer ring of the right hand bearing

Whilst the ball track was visible in the inner ring and in both the inner and outer ring of the left hand bearing, no sign of ball track was clearly visible on the outer ring of the right hand one

- Quantity and size of debris

The quantity and the size of the debris collected appeared excessive if compared with the wear visible on the lands of the right bearing

- Nature of the damaged spot in the outer ring and in the housing

The nature and possible origin of the damaged spot in the outer ring needed to be further analyzed and discussed to contribute to the identification of the initiation of the failure. In the following the additional findings are reported.

Cage
Although marks of interactions between balls and cage are present in several pockets, in correspondence of the maximum wear zone the ball pocket shows the strongest interaction marks with the ball, and an oval shape (Figure 13). Mainly one pocket shows this effect, while the roundness of the other ones is better maintained, indicating less severe ball-pocket interaction.
The inner side of the cage also shows light marks of interaction with the inner ring in a limited zone and diametrically opposed to the maximum wear on the outer side.

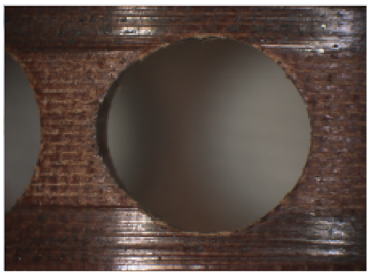

Figure 13: Pocket oval shape. Magnification x12

Inner ring
The brown zone, indicating the track of the balls is quite limited in width and the surface morphology of the track is not clearly distinguishable from the raceway when observed with the SEM (Figure 15). These two evidences indicate a likely low preload of the bearing. The different colour could be due to the deposit of some cage material on the surface.

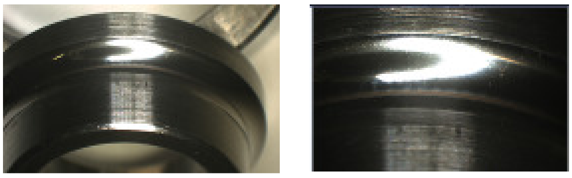

Figure 14: Ball track on inner ring.

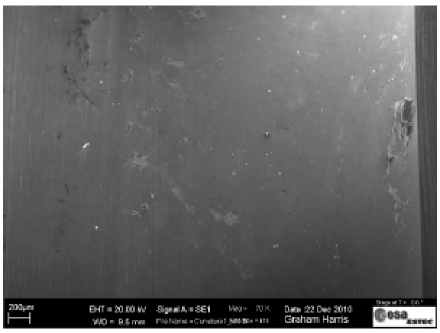

Figure 15: SEM image of the inner ring. The entire raceway is visible

4.1 Outer ring

The outer ring was in overall quite good condition and did not appear to have been affected by severe damage or wear, apart from the already mentioned lands' wear. The raceway of the balls appears in good condition. No evidence appears in the raceway of a ball track whatsoever (Figure 16).

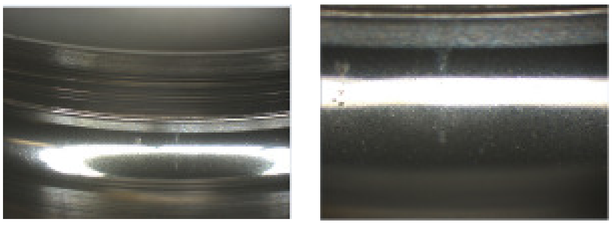

Figure 16: Outer ring worn lands and raceway

4.2 Dimensional measurements

The parts of the right hand bearing were measured using CMM with an overall measurement uncertainty for the cage, the outer ring and the inner ring of ± 0.002 mm (95% confidence)

Cage:

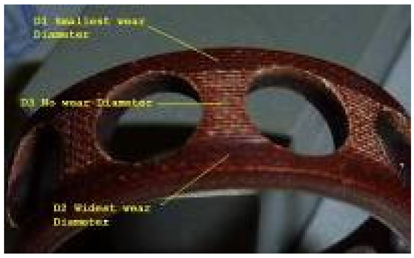

Figure 17: Cage different wear zones

Table 5: Cage dimensions of different wear zones

Cage dimensions	D1 (outer diameter worn)	D2 (outer diameter worn)	D3 (outer diameter unworn)	Inner diameter
Dimension (mm)	22.822	22.868	23.010	19.403
Out of roundness (mm)	0.140	0.122	0.035	0.033

It appears evident from the measurement that the diameters of the worn areas (D1 and D2) are affected by non negligible deviation indicated by the out of roundness value The outer diameter and the inner diameter have a better circular shape with very small displacements from roundness. This also confirms the small effect of the interaction between the cage and the inner ring

Balls
The balls diameter seems to indicate a variation of the balls size, and the potential presence of one or two balls bigger than the other ones, but this cannot be clearly stated, because, due to the uncertainty of the measurement, the diameters values are overall compatible.

4.3 Profile measurements

The cross section profiles of the cage and of the lands of the outer ring were measured using a profilometer. In the following the details of the results are reported

Cage

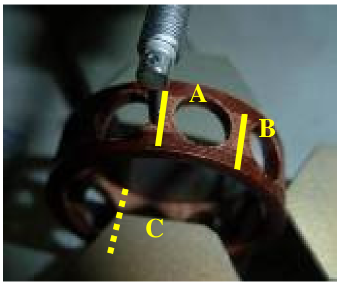

Figure 18: Profile measurements on the cage. A: profile next to the oval pocket. B: max wear step. C: min wear step

The profile was measured in three sections as indicated in Figure 18. It can be observed (Figure 19) that the wear is not equal on the two sides of the cage and appears bigger on the left hand side (140-150 µm) when compared to the right hand side (110-120 µm). The smallest wear is about 10-15 µm.

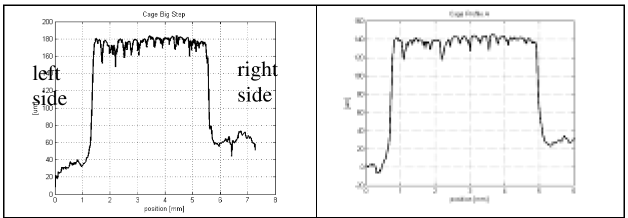

Figure 19: cage profile. Position B (upper left), position A (upper right)

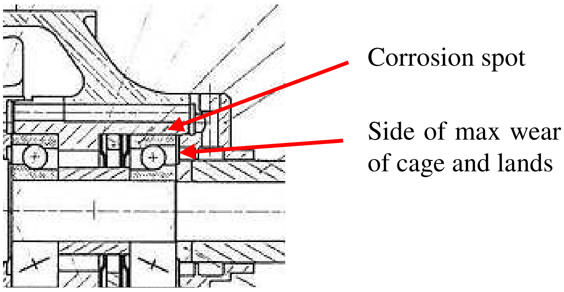

Figure 20: location of the biggest wear of the cage

The greater wear of the cage (left hand side in the profile plots) corresponds to the outer side of the right bearing in the assembly picture (Figure 20).

Outer ring

The worn lands of the two parts of the outer ring have been measured with the profilometer in the four locations indicated in Figure 21.

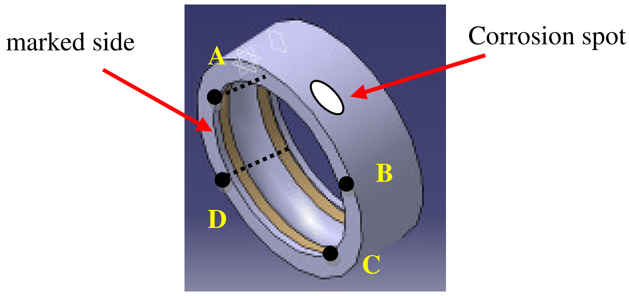

Figure 21: position of profile measurements on the outer ring

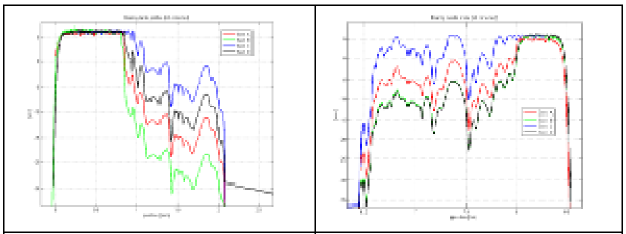

Figure 22: Profiles of the lands of the outer ring. A (red), B (green), C (blue), D (black) for both marked and non marked side

It can be observed (Figure 22) that the wear of the lands is not uniform over the circumference, and it ranges between roughly 10 µm (section C) to the max of 30 µm (section B). Moreover the maximum amplitude between peak and valley of the profile is of the order of 10 µm. The left hand side of the profiles (corresponding to the outer side of the bearing as indicated in Figure 20) shows a higher wear than the other side of the bearing.

It is worth to note the very good matching of the shape in all the profiles clearly indicating the same source of wear along the entire circumference, likely to be some particles entrapped between cage and outer ring clearance.

4.4 Debris

The debris collected while cleaning the parts were observed and examined using SEM.

From Fig. 17 it appears that the size of the debris collected is quite significantly large, reaching 80-100 µm in size. These dimensions appear to be inconsistent with the wear observed on the outer ring lands, in which the maximum amplitude of the peak-valley of the profile is 20 µm (see Figure 22).

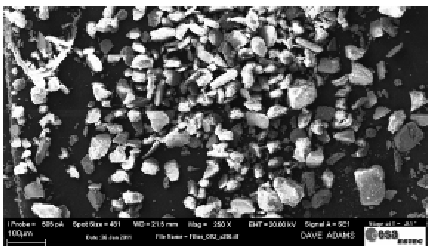

Figure 23: SEM analysis of debris. Outer ring

From the results of the components analysis of the debris samples (steel particles), only elements compatible with the composition of the steel of the bearing have emerged. It has to be noted that the difference in the composition of the bearing steel and the housing steel is quite subtle, mainly consisting in some percent in Ni content, therefore not easily detectable.
A clear statement cannot be made on the origin of these steel debris, while incompatibility in size with the wear of the lands is quite evident.

4.5 Outcomes summary

The left hand bearing did not show particular evidence of degradation. The most notable features are the light circumferential marks on the balls. The grease did not appear to be chemically contaminated, even if it appears darkened and with increased viscosity.

The right-hand bearing shows severe wear of the cage and the lands of the outer ring caused by strong interaction and high friction between these two parts.
It is speculated that at some point the bearing torque became so high that it exceeded the torque required to rotate the inner ring within its housing.
The outer ring has not been in the nominal position and free to move, as evidenced by different wear amount of the lands (tilted position) and by the matching corrosion spots in the outer diameter and in the housing. The presence of abrasive elements trapped between cage-outer ring clearance appear to be the only explanation of the severe damage on the lands.
The cage was pushed against the outer ring mainly by the effect of one ball, as suggested by the oval shape of one of the balls pockets.
Big bulky steel particles (up to 100 µm and more) found are not compatible with the lands wear grooves (10-15 µm).

The combination of the effects of a predominant ball guiding the cage, of the non nominal position of the outer ring with slight tilt, and of the decrease of the preload in the right bearing is in line with all the traces found. The non nominal position of the outer ring can bring about a low preload, that explains the light trace of the balls in the rings. A tilted position is consistent with the bigger wear found on the rightmost side both of the ring and of the cage. The non uniform circumferential wear of the cage and of the lands is consistent with a predominant interaction between one ball and the pocket.

5 PROBLEM UNDERSTANDING AND SUGGESTED SOLUTIONS

The non-nominal position of the outer ring and its inability to slide brought about a non-nominal preload on the bearings and an abnormal friction of the cage to the lands leading in the end to the failure of the fan.

The origin of the mispositioning of the bearing could be due to a sticking of the outer race within the housing due to fretting corrosion (vibrations), or also due to the intrusion of foreign particle through the clearance between bearing and housing. The last hypothesis appears to be the most likely, due to the morphology of the corrosion spot in the outer ring and housing.

The suggested solutions for the avoidance of the failure encountered are:

- Update procedures for handling of the bearing during assembly in order to avoid contamination of the outer surface that could lead to a corrosion blockage of the outer diameter against the housing
- Lubrication of the outer diameter of the bearing to facilitate its sliding if in contact with the housing, so to maintain its nominal position and preload

6 CONCLUSIONS

The work performed included a thorough investigation of a bearing assembly of the IRFA fan of the Columbus module on the ISS to identify the cause of its failure. The investigations included inspection and analysis using SEM, EDAX methods on the different parts and collected debris, and dimensional and profile measurements of the components.
The cause of the failure has been identified as a mispositioning (tilting) of the free-to-slide bearing that induced excessive cage-ring interaction with consequent wear and increase in friction that led to the premature failure

7 LESSONS LEARNED AND RECOMMENDATIONS

The following lessons learned can be highlighted:

- Where a bearing assembly design has a compliant preload system, the motion of the free-to-slide bearing must not be restricted
- Lubrication of the outer ring is recommended for this kind of solution to avoid possible sticking and/or tilt of the outer ring